Article

Structure

Crystal Structure of the CLOCK Transactivation Domain Exon19 in Complex with a Repressor

Graphical Abstract

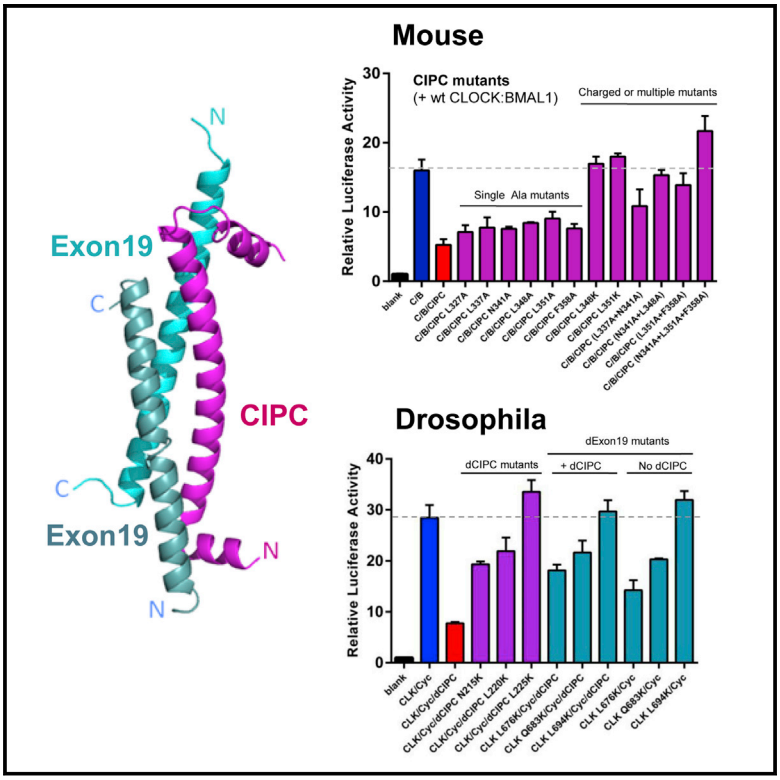

Highlights

- The X-ray structure of the transactivating Exon19 domain of CLOCK is determined
- CLOCK Exon19 and repressor CIPC form a coiled-coil complex with a 2:1 stoichiometry
- Exon19 interacts with both CIPC and coactivator(s) using overlapping interfaces
- Fly CIPC also interacts with Exon19 and represses CLK/CYC-mediated transcription

Authors

Zhiqiang Hou, Lijing Su, Jimin Pei, Nick V. Grishin, Hong Zhang

Correspondence

zhang@chop.swmed.edu

In Brief

Hou et al. report the structure of CLOCK transactivating Exon19 domain in complex with a repressor CIPC, providing the first insight into the structure mechanism of how CLOCK Exon19 interacts with a coregulator, and suggesting that CIPC function is conserved in *Drosophila* and other invertebrates.

Hou et al., 2017, Structure *25*, 1187–1194
August 1, 2017
http://dx.doi.org/10.1016/j.str.2017.05.023

Structure
Article

Crystal Structure of the CLOCK Transactivation Domain Exon19 in Complex with a Repressor

Zhiqiang Hou,[1,4] Lijing Su,[1,4] Jimin Pei,[2] Nick V. Grishin,[1,2,3] and Hong Zhang[1,3,5,*]
[1]Department of Biophysics
[2]Howard Hughes Medical Institute
[3]Department of Biochemistry
University of Texas Southwestern Medical Center, Dallas, TX 75390, USA
[4]These authors contributed equally
[5]Lead Contact
*Correspondence: zhang@chop.swmed.edu
http://dx.doi.org/10.1016/j.str.2017.05.023

SUMMARY

In the canonical clock model, CLOCK:BMAL1-mediated transcriptional activation is feedback regulated by its repressors CRY and PER and, in association with other coregulators, ultimately generates oscillatory gene expression patterns. How CLOCK:BMAL1 interacts with coregulator(s) is not well understood. Here we report the crystal structures of the mouse CLOCK transactivating domain Exon19 in complex with CIPC, a potent circadian repressor that functions independently of CRY and PER. The Exon19:CIPC complex adopts a three-helical coiled-coil bundle conformation containing two Exon19 helices and one CIPC. Unique to Exon19:CIPC, three highly conserved polar residues, Asn341 of CIPC and Gln544 of the two Exon19 helices, are located at the mid-section of the coiled-coil bundle interior and form hydrogen bonds with each other. Combining results from protein database search, sequence analysis, and mutagenesis studies, we discovered for the first time that CLOCK Exon19:CIPC interaction is a conserved transcription regulatory mechanism among mammals, fish, flies, and other invertebrates.

INTRODUCTION

Many organisms possess autonomous molecular clocks that coordinate their metabolism and behavior to have a ~24-hr period rhythm. The mammalian circadian clock is driven mainly by a negative transcription-translation feedback loop (Crane and Young, 2014; Lowrey and Takahashi, 2011). The positive arm of the loop is the heterodimeric CLOCK:BMAL1 transcriptional activator, which binds to the E-box (CACGTG) site at enhancer regions of clock-controlled genes and activates the expression of thousands of mammalian genes including those coding for their own repressors CRY and PER proteins (Gekakis et al., 1998; Koike et al., 2012) (Figure 1). The circadian transcription activator CLOCK:BMAL1 is reported to be a pioneer transcription factor able to bind specific DNA sites on nucleosomes (Menet et al., 2014). It recruits chromatin remodeling and modification enzymes and transcription coactivators, such as histone acetyltransferase (HAT) p300/CBP and histone methyltransferase MLL1 (Etchegaray et al., 2003; Katada and Sassone-Corsi, 2010; Menet et al., 2014), facilitates chromatin opening, and activates transcription of many genes (Figure 1). Repression of the CLOCK:BMAL1-mediated activation involves recruitment of specific transcription corepressors such as Sin3A and NurD histone deacetylase (HDAC) complexes by PER (Duong et al., 2011; Kim et al., 2014). The targeting of these corepressors to the CLOCK:BMAL1-specific sites is mediated through the tight association between PER and CRY (Nangle et al., 2014; Schmalen et al., 2014), as CRY is able to bind CLOCK:BMAL1 on and off DNA (Ye et al., 2011). Many other factors and enzymes regulate these processes through post-translational modifications of the core clock proteins such as phosphorylation, acetylation, and ubiquitination, to control protein-protein interactions and protein degradation, as well as nuclear-cytoplasmic transportation (Crane and Young, 2014; Mehra et al., 2009). Although many studies have shown that the core clock protein components interact with a number of factors in the general transcription machinery, little is known about the atomic details underlying these interactions. In particular, the exact domains or sequence motifs on coactivators that interact with CLOCK or BMAL1 have not been defined.

CLOCK and BMAL1 are basic helix-loop-helix and PER-ARNT-SIM (bHLH-PAS) domain-containing transcription factors (McIntosh et al., 2010; Moglich et al., 2009). We previously determined the crystal structure of the bHLH-PASAB domains of mouse CLOCK:BMAL1 heterodimer (Huang et al., 2012). These domains are responsible for dimerization and DNA binding, and are also critical for interacting with CRY and possibly other regulators. Both CLOCK and BMAL1 contain sequences C-terminal to the bHLH-PASAB domains that are important for transactivation. Specifically, a short C-terminal region of BMAL1 (residues 582–626) and the glutamine-rich regions of CLOCK, including the 51-residue domain encoded by *exon19* of the *Clock* gene (residues 514–564) were shown to be involved in transcription activation (Gekakis et al., 1998; Kiyohara et al., 2006; Takahata et al., 2000; Zhao et al., 2007). The Exon19 domain is important for mammalian circadian rhythm as demonstrated in the original study where the *Clock* gene was first identified by positional cloning (King et al., 1997). The *Clock* mutant mice had a distinct phenotype of longer circadian period, and their persistence of rhythmicity was abolished. At the molecular level, the *Clock* mutant resulted in an exon-skipping event and caused a deletion of 51 residues encoded by exon

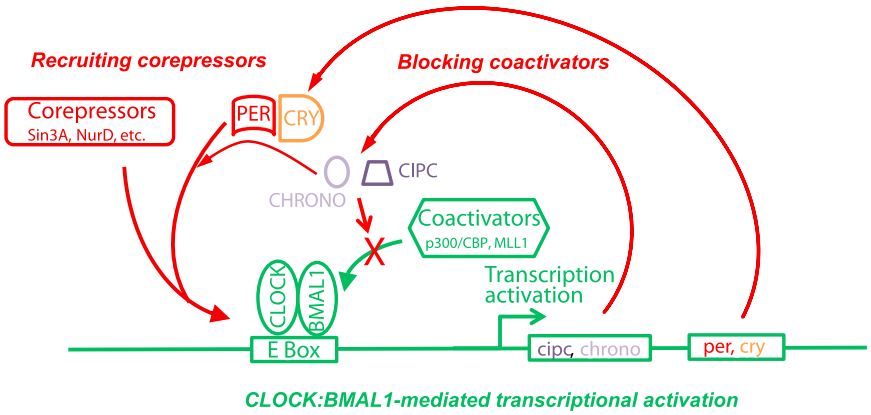

Figure 1. A Simplified Model of Mammalian Circadian Clock Feedback Loop

The transcriptional activating positive arm and its components (CLOCK:BMAL1 and coactivators) are colored green, whereas the negative arms are colored red. Two distinct negative transcriptional regulatory mechanisms are known: PER:CRY-mediated recruitment of corepressors and CIPC- or CHRONO-mediated blocking of coactivator interactions.

19 (King et al., 1997). CIPC protein was first identified in a yeast two-hybrid study to interact with CLOCK (Gekakis et al., 1998), and was later shown to specifically interact with the CLOCK Exon19 domain and repress CLOCK:BMAL1-mediated transactivation (Zhao et al., 2007), presumably by competitively masking the interactions between Exon19 and yet unidentified protein factors/domains required for transactivation. The action of CIPC is independent of CRY and PER (Zhao et al., 2007). Together with other CRY- and PER-independent repressors such as the recently identified CHRONO (Anafi et al., 2014; Annayev et al., 2014; Goriki et al., 2014), the clock feedback loop appears to have additional negative arms regulating clock-mediated transactivation through different mechanisms from that of CRY and PER (Figure 1).

RESULTS

Structure Determination of the Mouse CLOCK Exon19:CIPC Complex

To understand the structural basis of CLOCK Exon19 function, we set out to determine the three-dimensional structure of Exon19 in complex with CIPC. Because of the small size of Exon 19 (51 amino acids) and the predicted coiled-coil helical structure, we reasoned that Exon19 by itself might not be stable and would need its binding partner to achieve a well-folded compact conformation. We made three different constructs to coexpress CLOCK Exon19 domain and CIPC C-terminal region that interacts with Exon19 (CIPC-C) (Figures 2A and S1A). As expected, when expressed alone, Exon19 and CIPC-C were insoluble and existed in the inclusion body. They became soluble when coexpressed, and the complex can be readily purified. The purified Exon19:CIPC-C complex from one of our constructs, Exon19 (residues 517–560) and CIPC-C (residues 317–379), has well-dispersed $^{1}H,^{15}N$ HSQC (heteronuclear single-quantum coherence) spectra (Figure S1B) and the protein was readily crystallized. Two crystal forms were obtained in different crystallization conditions. We determined the Exon19:CIPC-C structure in both forms by a single-wavelength anomalous diffraction (SAD) phasing method using selenomethionine protein crystals. The structure of the orthorhombic $P2_12_12_1$ form was determined first and refined to the resolution of 1.86 Å (Table 1 and Figure S2).

Overall Structure

Both Exon19 and CIPI-C adopt a long-helical conformation and form a coiled-coil bundle as predicted (Figure 2B). However, to our surprise, the bundle contains three helices with a stoichiometry of two Exon19 and one CIPC (Figure 2B). The Exon19

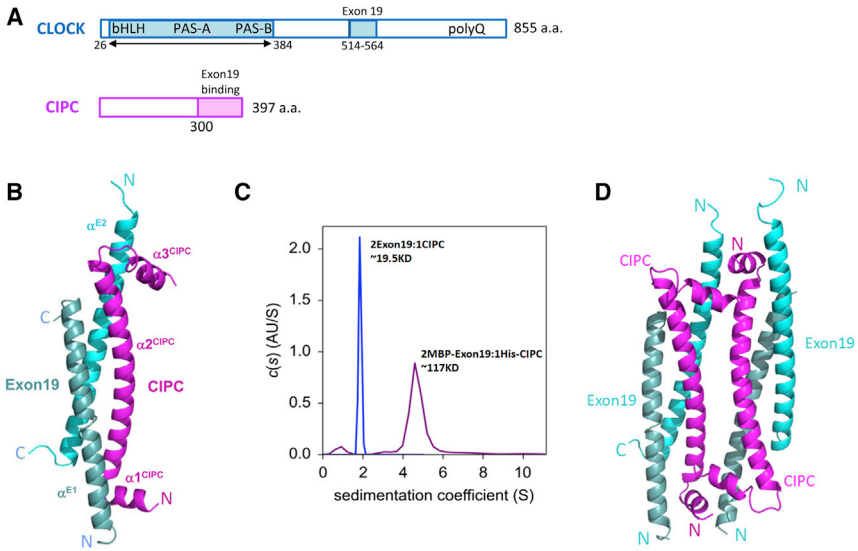

Figure 2. Structure of CLOCK Exon19:CIPC Complex

(A) Domain organizations of mouse CLOCK and CIPC. a.a., amino acids.

(B) The coiled-coil three-helical bundle structure of Exon19:CIPC with 2:1 stoichiometry.

(C) Sedimentation-velocity ultracentrifugation analyses of Exon19:CIPC complexes. The experimentally deduced molecular weights (MW) closely match those calculated for the complexes with two Exon19 and one CIPC stoichiometry. For the untagged 2:1 complex, the calculated MW is 19.1 kDa. The tagged 2:1 complex has a calculated MW of 113 kDa.

(D) The dimerization of two 2:1 Exon19:CIPC three-helical bundle in the crystal.

Table 1. X-Ray Data Collection and Refinement Statistics

	Crystal I	Crystal II
Data Collection		
Space group	$P2_12_12_1$	C_2
Cell dimensions		
a, *b*, *c* (Å)	24.34, 77.58, 150.36	175.5, 116.8, 132.9
α, β, γ (°)	90.00, 90.00, 90.00	90.00, 126.5, 90.00
Resolution (Å)	50.0–1.86 (1.89–1.86)[a]	50–2.70 (2.75–2.70)[a]
R_{sym} or R_{merge}	0.079	0.087
$I/\sigma I$	28.6 (1.2)	16.1 (1.1)
Completeness (%)	97.7 (90.2)	99.9 (99.1)
Redundancy	9.2 (4.9)	5.7 (4.5)
Unique reflections	24,841	59,416
Refinement		
Resolution (Å)	50.0–1.86	50–2.70
No. of reflections	22,684	53,213
R_{work}/R_{free}	0.210/0.262	0.218/0.275
No. of atoms		
Protein	2,438	12,247
Water	199	338
B factors		
Protein	25.1	26.2
Water	38.3	36.9
RMSDs		
Bond lengths (Å)	0.010	0.014
Bond angles (°)	1.023	1.429
Ramachandran plot[b]		
Favored regions (%)	99.3	98.5
Outliers (%)	0	0

[a]Values in parentheses represent highest-resolution shell.
[b]Evaluated by MolProbity.

domain adopts the structure of a single long helix and the two Exon19 helices run anti-parallel to each other with a slight right-handed superhelical twist. We name these two helices from the two Exon19 molecules in the complex α^{E1} and α^{E2}, respectively. The CIPC-C domain contains three helices: a central long α helix, $\alpha2^{CIPC}$, which docked to the concaved surface generated by the two Exon19 helices, and two short helices, $\alpha1^{CIPC}$ and $\alpha3^{CIPC}$, capping the N and C termini of the central $\alpha2^{CIPC}$ helix (Figure 2B). The N-terminal $\alpha1^{CIPC}$ runs roughly perpendicular to the central $\alpha2^{CIPC}$and interacts with the N-terminal section of the first Exon19 α^{E1}. The C-terminal $\alpha3^{CIPC}$, on the other hand, runs at an angle ~60° to the central $\alpha2^{CIPC}$ and contacts the N-terminal section of the second Exon19 helix α^{E2}. This $\alpha3^{CIPC}$ helix is important for the stability of the complex, as one of our coexpression constructs lacking this helix is unstable (data not shown).

CLOCK Exon19:CIPC Complex Has a 2:1 Stoichiometry in Solution

To assess that Exon19 and CIPC indeed exist as a 2:1 complex in solution, we performed analytical ultracentrifugation (AUC) experiments on the coexpressed tag-free Exon19:CIPC-C complex and on the maltose binding protein (MBP)-Exon19:CIPC-C complex, where Exon19 is fused at the N terminus to the 41-kDa MBP. The results obtained for both samples (Figure 2C) indicated that the complex indeed has two Exon19 and one CIPC-C in either untagged or MBP-tagged form. In addition, we have obtained another crystal form of the complex in the C2 space group from a different crystallization condition and have solved the crystal structure of this second crystal form (Table 1). Despite completely different crystal lattice packing, the C2 structure also has the same 2:1 stoichiometry and very similar three-helical bundle conformation (root-mean-square deviation [RMSD] between C_α atoms of the heterotrimeric complexes in the two crystals is 0.87 Å). In both crystal forms, a dimer of the 2:1 Exon19:CIPC heterotrimers is also observed (Figure 2D). However, higher oligomerization states were not observed in solution in the AUC experiments. Therefore, it appears that only at a much higher Exon19 and CIPC concentration, such as in crystals, does a dimer of the trimeric complexes become possible.

Interactions between CLOCK Exon19 and CIPC

The Exon19:CIPC interface at the coiled-coil three-helical bundle region may be divided into three segments (Figure 3A). The first segment (I) runs from residues L330 to L337 of CIPC $\alpha2^{CIPC}$, L530 to I537 of Exon19 α^{E1}, and L548 to L555 of α^{E2}, containing about two helical turns and a small hydrophobic core. Interestingly, the mid-section of the three-helical bundle (segment II) is mostly hydrophilic, running from N341 to Q345 of CIPC $\alpha2^{CIPC}$, and from N540 to Q545 of both Exon19 helices. The CIPC Asn341 side chain forms bifurcated hydrogen bonds with the side chains of the two Exon19 Gln544 residues at this interface. The third segment (III), running from L348 to T362 on the CIPC helix $\alpha2^{CIPC}$, is about 3.5 α-helical turns long and is packed against the hydrophobic regions of the two Exon19 helices (L548 to L555 of Exon19 α^{E1}, and L526 to I537 of α^{E2}). This segment of the bundle (III) has a larger hydrophobic core. Additionally the C-terminal helix of CIPC ($\alpha3^{CIPC}$) makes hydrophobic contacts with the N-terminal segment of the second Exon19 molecule: L373 and L377 of CIPC are within van der Waals interaction distance to M523 and L526 of Exon19 α^{E2} (Figure 3A).

Structure-based mutagenesis analysis showed that the interface between Exon19 and CIPC observed in crystal structures is indeed important for the CIPC repression function in cells (Figures 3B and 3C). First, we systematically mutated a number of interface residues on CIPC and measured whether these CIPC mutants were still able to repress CLOCK:BMAL1-mediated transactivation in a mouse *Per2* promoter-driven Luciferase reporter assay (Figure 3B). Wild-type (wt) CIPC significantly inhibits activation mediated by CLOCK:BMAL1 to the same extent as if the CLOCK Exon19 is deleted (~25%–30% of wt CLOCK:BMAL1 activity in the absence of CIPC) (Figure 3C). A number of CIPC single Ala mutants at the hydrophobic interface, e.g., L327A, L337A, N341A, L348A, L351A, and F358A, are slightly less repressive than wt CIPC (~50% wt CLOCK:BMAL1 activation). However, the charged mutants L348K and L351K, as well as some of the double or triple mutants, fully restored transactivation by CLOCK:BMAL1, suggesting that these CIPC mutants no longer bind to Exon19 and repress CLOCK function. In the

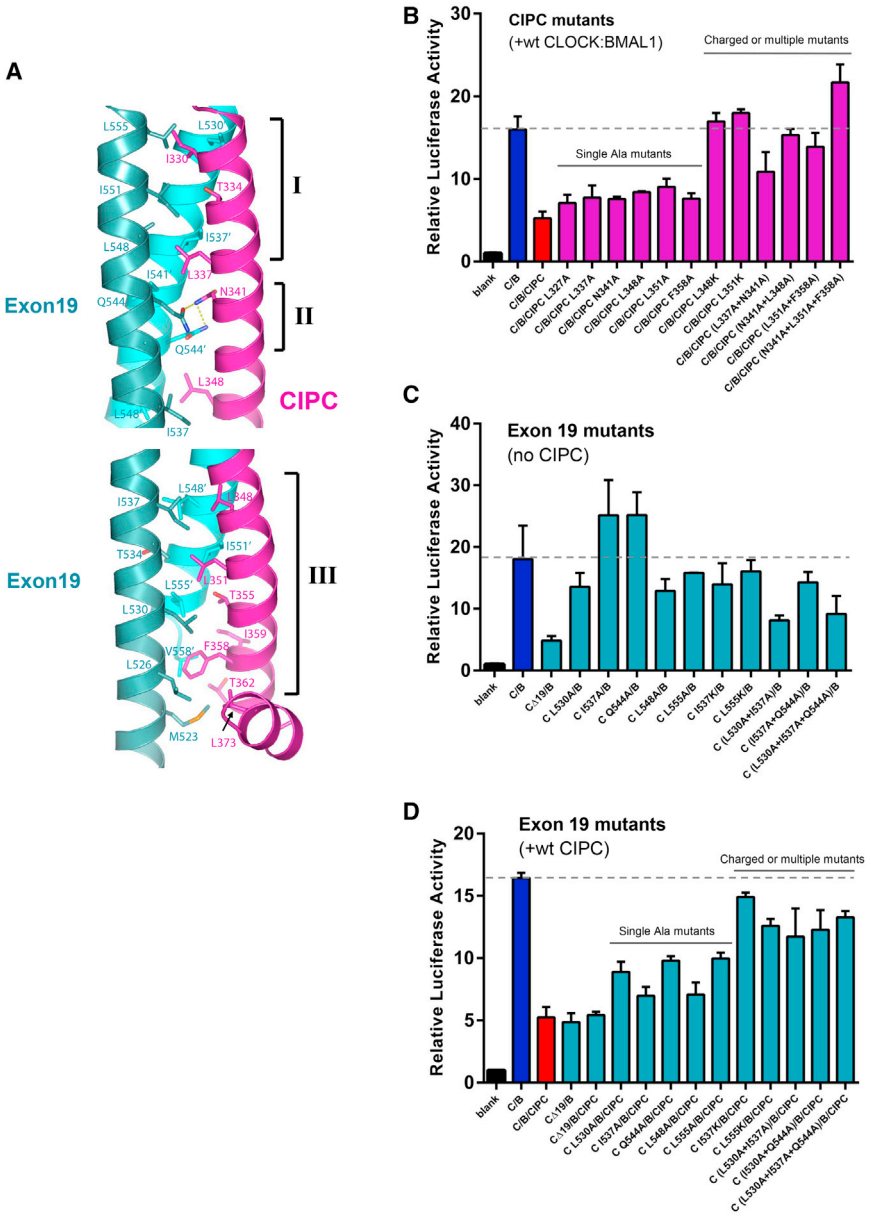

Figure 3. Interface between CLOCK Exon19 and CIPC

(A) Details of Exon19 and CIPC interface at the interior of the coiled-coil three-helical bundle with side chains of relevant residues, shown in stick representation. The bundle is broken up into two parts with different viewing angles for clarity. The three distinct segments are marked I, II, and III.

(B) A *Per2* promoter-driven Luciferase reporter assay was used to evaluate the effects of CIPC mutants on its repression activities. Cells were transfected with wide-type CLOCK and BMAL1 and with either wild-type or mutant CIPC as indicated.

(C) Effects of selected CLOCK Exon19 mutants on the CLOCK:BMAL1-mediated transactivation in the reporter assays.

(D) Effects of Exon19 mutants on the CIPC-mediated repression of CLOCK:BMAL1 activity.

Data in (B) to (D) are presented as mean ± SD of three replicates in a single assay. The results shown are representative of at least three independent experiments.

case of Exon19 mutants, we take into consideration that the same Exon19 surface may interact with both coactivators and CIPC. Therefore, we first evaluated whether these Exon19 mutants affected transactivation in the absence of CIPC. Some of the single Exon19 mutants, L530A, L548A, L555A, I537K, and L555K have slightly reduced activity (~70%–80% of wt CLOCK:BMAL1 activity) (Figure 3C), whereas I537A and Q544A have increased activity. The double or triple Exon19 mutants would have more significantly reduced activity, about 40% of the wild-type protein. These data suggest that these Exon19 residues, which are in contact with CIPC in our crystal structures, likely are also involved in recruiting coactivators and activating transcription in the absence of CIPC. In the presence of CIPC, these single Exon19 mutants (L530A, I537A, Q544A, L548A, and L555A) were able to be repressed by CIPC (~50% wt CLOCK:BMAL1 activity compared with 70%–80% in the absence of CIPC) (Figure 3D). For the charged mutants (I537K and L555K) and double/triple Ala mutants, the repression is nearly abolished (~70% activity, similar to that of Exon19 mutant alone in the absence of CIPC). These results strongly suggest that the same or largely overlapping regions on Exon19 interact with both coactivator(s) and CIPC.

Exon19:CIPC Interaction Is a Conserved Transcription Regulation Mechanism in *Drosophila*

Database searches for protein sequences homologous to Exon19 and CIPC indicate that Exon19 is a conserved motif of CLOCK in both vertebrate and invertebrate species (Figure 4). Moreover, CIPC homologs have a phylogenetic distribution similar to that of CLOCK Exon19 (Figure 4). To test whether fly CLOCK Exon19-homologous region also interacts with fly CIPC, we coexpressed recombinant fly CLOCK (dCLK) Exon19-like domain (we will call this simply "dCLK Exon19" for short) and fly CIPC C-terminal domain (accession number GenBank: AAF56571.2). The result shows that indeed they form a stable complex and can be copurified (Figure 5A). Analytical ultracentrifugation analyses of purified fly Exon19:CIPC complex indicate that it also has the same 2:1 stoichiometry as the mouse complex in solution (Figure S3). Moreover, dCIPC is able to repress dCLK:CYC-mediated transcription activation effectively (Figure 5B). Site-directed mutagenesis results suggest that the same or at least similar regions on both mCIPC and dCIPC are involved in interacting with the CLOCK transactivating domain, because when these residues, for example, dCIPC residues Asn215, Leu222, and Leu225 (corresponding

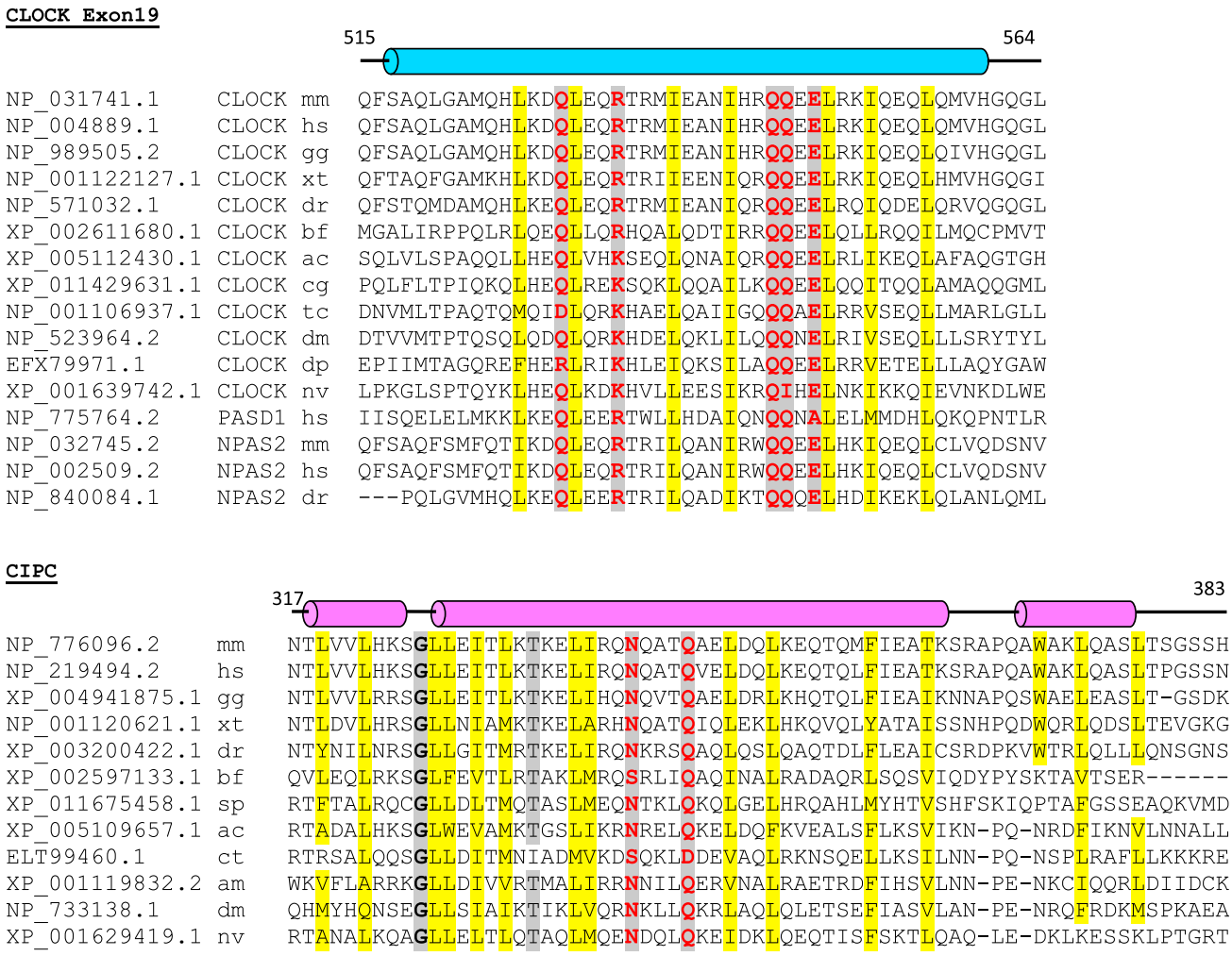

Figure 4. Multiple Sequence Alignments of the CLOCK Exon19 Domains and CIPC Homologs from Representative Species

The accession number and species abbreviation are listed at the beginning of each sequence. mm, *Mus musculus*; hs, *Homo sapiens*; gg, *Gallus gallus*; xt, *Xenopus tropicalis*; dr, *Danio rerio*; bf, *Branchiostoma floridae*; ac, *Aplysia californica*; cg, *Crassostrea gigas*; tc, *Tribolium castaneum*; dm, *Drosophila melanogaster*; dp, *Daphnia pulex*; nv, *Nematostella vectensis*; sp, *Strongylocentrotus purpuratus*; ct, *Capitella teleta*; ap, *Apis mellifera*. Conserved hydrophobic residues are highlighted in yellow; conserved polar residues are bold on gray. The mammalian NPAS2 proteins are CLOCK paralogs enriched in brain. PASD1 is a cancer/testis antigen protein containing an Exon19 homologous domain (shown here) and was recently reported to repress clock-mediated transcription (Liggins et al., 2004; Michael et al., 2015).

to mouse CIPC Asn341, L348, and Leu351, respectively, Figure 5C) are mutated to a charged lysine residue, the resulted mutant dCIPC no longer repress dCLK/CYC as efficiently as the wt dCIPC (Figure 5B). In particular, the dCIPC L225K mutant lost the repressive activity completely, similar to the effect caused by the corresponding mouse CIPC L351K mutant (Figure 3A). Mutations of dCLK Exon19 residues Leu676 and Gln683 (corresponding to mouse CLOCK Ile537 and Gln544) to a lysine residue decreased dCLK/CYC-mediated transactivation (Figure 5B), suggesting that these residues may be involved in interacting with coactivators, like those on mouse CLOCK. However, dCLK Exon19 mutant L694K (corresponding to mouse CLOCK L555K) has essentially no effect on the transactivation (or may even have a slightly increased transactivation). This is somewhat different from the corresponding mouse CLOCK mutant L555K, which has a slightly decreased activity. These observations suggest that dCLK Exon19 should have a function similar to that of mouse CLOCK Exon19 in recruiting transcription coactivators, although the detailed mechanism may differ. Furthermore, the presence of dCIPC does not affect the outcome of these dCLK Exon19 mutants (Figure 5B). These results strongly suggest that while the CLOCK Exon19 domains in both mouse and *Drosophila* are involved in transactivation and can be repressed by CIPC, the detailed mechanisms may differ and need to be further investigated.

DISCUSSION

In the present study, we determined the high-resolution crystal structure of the CLOCK transactivation domain Exon19 in complex with repressor CIPC. The complex adopts a coiled-coil three-helical bundle conformation with a stoichiometry of two

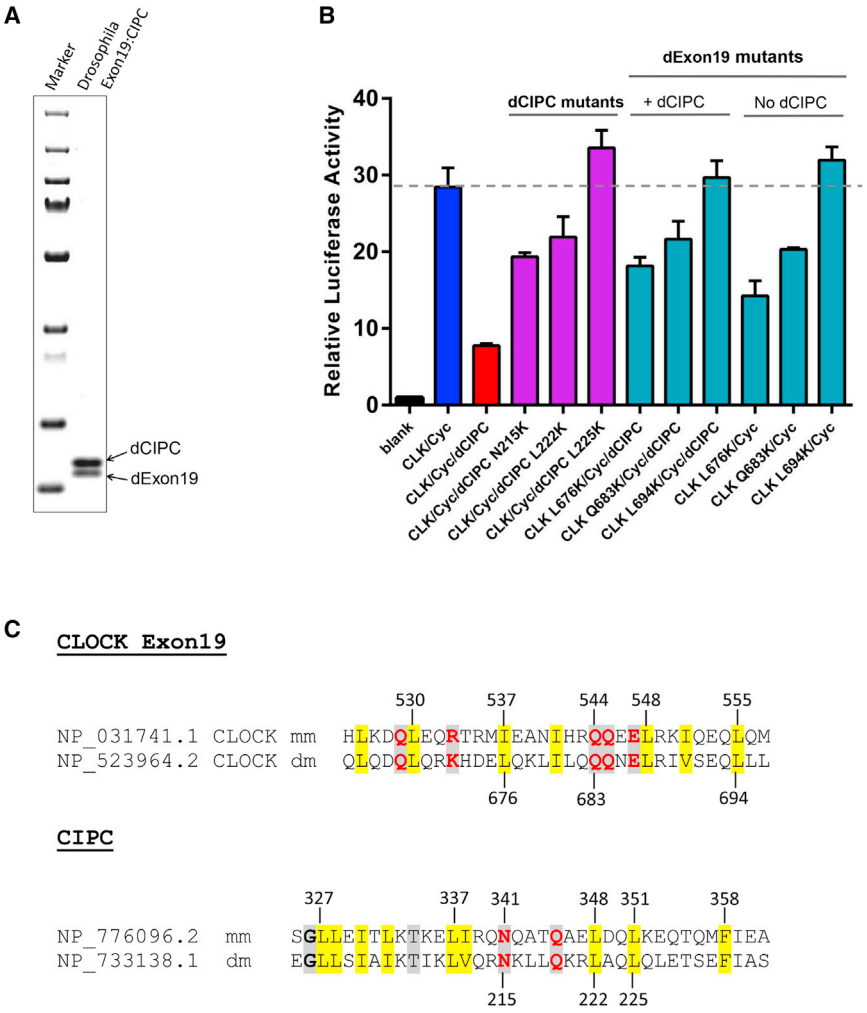

Figure 5. Interaction between CLOCK Exon19 and CIPC Is Conserved in *Drosophila*

(A) The Exon19 domain of dCLK (dExon19) and the C-terminal domain of dCIPC were coexpressed in *Escherichia coli* and copurified by Ni-NTA affinity and size-exclusion chromatography.

(B) *Drosophila* CIPC represses CLK:CYC-mediated transcription activation in S2 cells. CLK and CYC are *Drosophila* homologs of mammalian CLOCK and BMAL1, respectively.

(C) Pairwise alignment of mouse and *Drosophila* Exon19 and CIPC sequences in the helical bundle region. The mutated residue numbers are marked above for mouse residues and below for *Drosophila* residues.

Exon19 and one CIPC. To our knowledge, such an intermolecular coiled-coil interface has not been observed between other transcription activators with either coactivator or corepressor. The three-dimensional structures of a number of transactivation domains (TADs) of transcription activators have been characterized in complex with their partners, either a coactivator or a corepressor. These include the TAD domain of p53, CREB, or HIFα in complex with the TAZ or KIX domains of p300/CBP (Feng et al., 2009; Freedman et al., 2002, 2003; Radhakrishnan et al., 1997; Wang et al., 2012; Wojciak et al., 2009), among others. The coiled-coil interface as observed between Exon19 and CIPC appears to be unique. Although the function of the CIPC homologs in other species has not been annotated thus far, gene expression profiling studies in *Drosophila melanogaster* showed that the transcript encoding fly CIPC homolog, CG31324, was significantly enriched in fly clock cells (Nagoshi et al., 2010). In the present work, we have shown that fly CIPC interacts directly and tightly with the dCLK Exon19 domain as they can be coexpressed and copurified together as a stable complex. Because dCIPC is able to repress dCLK:CYC-mediated transcription activation effectively (Figure 5B), we propose that it also plays a role in fly circadian clock regulation similar to that of mammalian CIPC.

CLOCK:BMAL1 has been shown to interact with a number of transcription coactivators, such as histone acetyltransferase p300/CBP and histone methyltransferase MLL1 (Etchegaray et al., 2003; Katada and Sassone-Corsi, 2010), through their C-terminal TADs. In addition to Exon19, a C-terminal helical domain of BMAL1 is also involved in recruiting coactivators (Kiyohara et al., 2006), which explains why deletion of Exon19 does not completely abolish CLOCK:BMAL1-mediated transcription activation. As a pioneer transcription activator, CLOCK:BMAL1 binds E-box DNA on chromosome, and recruits these chromatin-modifying factors to facilitate chromatin opening and activate transcription globally (Menet et al., 2014). However, so far the specific domains within either p300/CBP or MLL1 that interact with CLOCK:BMAL1 have not been identified. The crystal structure of CLOCK Exon19:CIPC complex provided for the first time a structural mechanism underlying Exon19-mediated protein-protein interactions. It should be helpful to use such knowledge to search for the coiled-coil regions in transcription coactivators that may interact with Exon19. Notably, the interaction between Exon19 and CIPC is highly specific. In addition to the leucine-zipper type of sequences typical of coiled-coil helices, a polar residue, Asn341, on CIPC or other potential Exon19-interacting proteins, at the middle of the helix should be important for the stability of the complex.

The 2:1 stoichiometry of Exon19:CIPC complex is intriguing and suggests that CIPC can only inhibit CLOCK:BMAL1 when there are at least two activator complexes binding at the adjacent promoter/enhancer region (Figure 6). Clustering of transcription factor binding sites is common for many transcription activators including E boxes recognized by CLOCK:BMAL1 (Berman et al., 2002; Rey et al., 2011). Tandem E boxes often exist in the same regulatory region, and binding of multiple copies of the CLOCK:BMAL1 usually leads to enhanced gene transcription activation. Because of the pioneer characteristics of CLOCK:BMAL1, E boxes distant in DNA sequence could also be spatially close due to the compact chromatin structure,

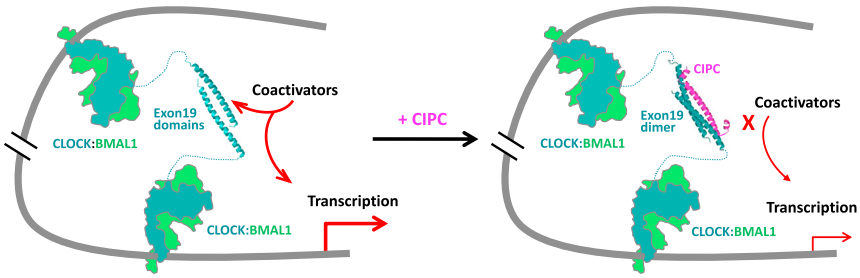

Figure 6. Proposed Mechanism of Exon19 Domain Action and CIPC-Mediated Repression of CLOCK:BMAL1

In the absence of CIPC, binding to the tandem E boxes on DNA would bring two or more CLOCK:BMAL1 activators in proximity and enable a more effective recruitment of general coactivators by CLOCK Exon19 domains. Interaction with CIPC induces the formation of the 2:1 Exon19:CIPC complex and would interfere with the coactivator recruitment thus repress CLOCK:BMAL1-mediated transactivation.

allowing two CLOCK:BMAL1 complexes and, thus, two Exon19 helices to come close together to interact with coactivators or be inhibited by specific repressors such as CIPC (Figure 6). We further speculate that Exon19 helix may be a versatile structure module for interacting with different protein partners and could form different coiled-coil helical bundle complexes depending on with which protein partner it interacts. Further identification of Exon19-interacting protein domains and structural characterization of Exon19 in complex with these proteins will provide much-needed insights into the transactivation mechanisms of CLOCK.

STAR★METHODS

Detailed methods are provided in the online version of this paper and include the following:

- KEY RESOURCES TABLE
- CONTACT FOR REAGENT AND RESOURCE SHARING
- EXPERIMENTAL MODEL AND SUBJECT DETAILS
  - HEK293T Cell Culture
  - Schneider 2 (S2) Cell Culture
- METHOD DETAILS
  - Protein Expression, Purification, and Crystallization
  - X-Ray Data Collection, Structure Determination and Analysis
  - Analytical Ultracentrifuge
  - ^{15}N-^{1}H TROSY-HSQC
  - Mutagenesis
  - Transactivation Assays
- DATA AND SOFTWARE AVAILABILITY

SUPPLEMENTAL INFORMATION

Supplemental Information includes three figures and can be found with this article online at http://dx.doi.org/10.1016/j.str.2017.05.023.

AUTHOR CONTRIBUTIONS

Z.H., L.S., and H.Z. designed experiments. Z.H. and L.S. performed experiments. J.P. performed bioinformatics analysis. Z.H., L.S., N.V.G., and H.Z. analyzed the data and wrote the manuscript.

ACKNOWLEDGMENTS

This research is supported by the NIH (R01 GM104496 to H.Z.) and the Welch Foundation (I-1505 to N.V.G.). We thank Drs. Jose-Rizo-Rey and Qiong Wu for help with the NMR experiments; Drs. Diana Tomchick and James Chen for help with synchrotron data collection; Drs. Thomas Scheuermann and Chad Brautigam for help with the analytical ultracentrifugation experiments; Drs. Cheng-Ming Chiang and Shwu-Yuan Wu for advice on transactivation assays; and Dr. Shuang Li for S2 cell firefly luciferase assay. We are grateful to Dr. Chuck Weitz for advice on CIPC repression assays; Dr. Bruce Beutler for the use of cell culture and Luciferase Reporter Assay System; and UT Southwestern Proteomics Core facility for their services. Results shown in this report are derived from work performed at Argonne National Laboratory, Structural Biology Center at Advanced Photon Source. Argonne is operated by UChicago Argonne, LLC, for the U.S. Department of Energy, Office of Biological and Environmental Research under contract DE-AC02-06CH11357.

Received: February 20, 2017
Revised: May 4, 2017
Accepted: May 25, 2017
Published: June 29, 2017

REFERENCES

Adams, P.D., Afonine, P.V., Bunkoczi, G., Chen, V.B., Davis, I.W., Echols, N., Headd, J.J., Hung, L.W., Kapral, G.J., Grosse-Kunstleve, R.W., et al. (2010). PHENIX: a comprehensive Python-based system for macromolecular structure solution. Acta Crystallogr. D Biol. Crystallogr. *66*, 213–221.

Anafi, R.C., Lee, Y., Sato, T.K., Venkataraman, A., Ramanathan, C., Kavakli, I.H., Hughes, M.E., Baggs, J.E., Growe, J., Liu, A.C., et al. (2014). Machine learning helps identify CHRONO as a circadian clock component. PLoS Biol. *12*, e1001840.

Annayev, Y., Adar, S., Chiou, Y.Y., Lieb, J.D., Sancar, A., and Ye, R. (2014). Gene model 129 (Gm129) encodes a novel transcriptional repressor that modulates circadian gene expression. J. Biol. Chem. *289*, 5013–5024.

Berman, B.P., Nibu, Y., Pfeiffer, B.D., Tomancak, P., Celniker, S.E., Levine, M., Rubin, G.M., and Eisen, M.B. (2002). Exploiting transcription factor binding site clustering to identify cis-regulatory modules involved in pattern formation in the *Drosophila* genome. Proc. Natl. Acad. Sci. USA *99*, 757–762.

Collaborative Computational Project, Number 4 (1994). The CCP4 suite—programs for protein crystallography. Acta Crystallogr. D Biol. Crystallogr. *50*, 760–763.

Crane, B.R., and Young, M.W. (2014). Interactive features of proteins composing eukaryotic circadian clocks. Annu. Rev. Biochem. *83*, 191–219.

Davis, I.W., Murray, L.W., Richardson, J.S., and Richardson, D.C. (2004). MOLPROBITY: structure validation and all-atom contact analysis for nucleic acids and their complexes. Nucleic Acids Res. *32*, W615–W619.

Delaglio, F., Grzesiek, S., Vuister, G.W., Zhu, G., Pfeifer, J., and Bax, A. (1995). NMRPipe: a multidimensional spectral processing system based on UNIX pipes. J. Biomol. NMR *6*, 277–293.

Duong, H.A., Robles, M.S., Knutti, D., and Weitz, C.J. (2011). A molecular mechanism for circadian clock negative feedback. Science *332*, 1436–1439.

Emsley, P., Lohkamp, B., Scott, W.G., and Cowtan, K. (2010). Features and development of Coot. Acta Crystallogr. D Biol. Crystallogr. *66*, 486–501.

Etchegaray, J.P., Lee, C., Wade, P.A., and Reppert, S.M. (2003). Rhythmic histone acetylation underlies transcription in the mammalian circadian clock. Nature *421*, 177–182.

Feng, H., Jenkins, L.M., Durell, S.R., Hayashi, R., Mazur, S.J., Cherry, S., Tropea, J.E., Miller, M., Wlodawer, A., Appella, E., et al. (2009). Structural basis for p300 Taz2-p53 TAD1 binding and modulation by phosphorylation. Structure *17*, 202–210.

Freedman, S.J., Sun, Z.Y., Poy, F., Kung, A.L., Livingston, D.M., Wagner, G., and Eck, M.J. (2002). Structural basis for recruitment of CBP/p300 by hypoxia-inducible factor-1 alpha. Proc. Natl. Acad. Sci. USA *99*, 5367–5372.

Freedman, S.J., Sun, Z.Y., Kung, A.L., France, D.S., Wagner, G., and Eck, M.J. (2003). Structural basis for negative regulation of hypoxia-inducible factor-1alpha by CITED2. Nat. Struct. Biol. *10*, 504–512.

Gekakis, N., Staknis, D., Nguyen, H.B., Davis, F.C., Wilsbacher, L.D., King, D.P., Takahashi, J.S., and Weitz, C.J. (1998). Role of the CLOCK protein in the mammalian circadian mechanism. Science *280*, 1564–1569.

Goriki, A., Hatanaka, F., Myung, J., Kim, J.K., Yoritaka, T., Tanoue, S., Abe, T., Kiyonari, H., Fujimoto, K., Kato, Y., et al. (2014). A novel protein, CHRONO, functions as a core component of the mammalian circadian clock. PLoS Biol. *12*, e1001839.

Hao, H., Allen, D.L., and Hardin, P.E. (1997). A circadian enhancer mediates PER-dependent mRNA cycling in *Drosophila melanogaster*. Mol. Cell. Biol. *17*, 3687–3693.

Huang, N., Chelliah, Y., Shan, Y., Taylor, C.A., Yoo, S.H., Partch, C., Green, C.B., Zhang, H., and Takahashi, J.S. (2012). Crystal structure of the heterodimeric CLOCK: BMAL1 transcriptional activator complex. Science *337*, 189–194.

Johnson, B.A., and Blevins, R.A. (1994). NMR View: a computer program for the visualization and analysis of NMR data. J. Biomol. NMR *4*, 603–614.

Katada, S., and Sassone-Corsi, P. (2010). The histone methyltransferase MLL1 permits the oscillation of circadian gene expression. Nat. Struct. Mol. Biol. *17*, 1414–1421.

Kim, J.Y., Kwak, P.B., and Weitz, C.J. (2014). Specificity in circadian clock feedback from targeted reconstitution of the NuRD corepressor. Mol. Cell *56*, 738–748.

King, D.P., Zhao, Y., Sangoram, A.M., Wilsbacher, L.D., Tanaka, M., Antoch, M.P., Steeves, T.D., Vitaterna, M.H., Kornhauser, J.M., Lowrey, P.L., et al. (1997). Positional cloning of the mouse circadian clock gene. Cell *89*, 641–653.

Kiyohara, Y.B., Tagao, S., Tamanini, F., Morita, A., Sugisawa, Y., Yasuda, M., Yamanaka, I., Ueda, H.R., van der Horst, G.T., Kondo, T., et al. (2006). The BMAL1 C terminus regulates the circadian transcription feedback loop. Proc. Natl. Acad. Sci. USA *103*, 10074–10079.

Koike, N., Yoo, S.H., Huang, H.C., Kumar, V., Lee, C., Kim, T.K., and Takahashi, J.S. (2012). Transcriptional architecture and chromatin landscape of the core circadian clock in mammals. Science *338*, 349–354.

Liggins, A.P., Brown, P.J., Asker, K., Pulford, K., and Banham, A.H. (2004). A novel diffuse large B-cell lymphoma-associated cancer testis antigen encoding a PAS domain protein. Br. J. Cancer *91*, 141–149.

Lowrey, P.L., and Takahashi, J.S. (2011). Genetics of circadian rhythms in Mammalian model organisms. Adv. Genet. *74*, 175–230.

McIntosh, B.E., Hogenesch, J.B., and Bradfield, C.A. (2010). Mammalian Per-Arnt-Sim proteins in environmental adaptation. Annu. Rev. Physiol. *72*, 625–645.

Mehra, A., Baker, C.L., Loros, J.J., and Dunlap, J.C. (2009). Post-translational modifications in circadian rhythms. Trends Biochem. Sci. *34*, 483–490.

Menet, J.S., Pescatore, S., and Rosbash, M. (2014). CLOCK: BMAL1 is a pioneer-like transcription factor. Genes Dev. *28*, 8–13.

Michael, A.K., Harvey, S.L., Sammons, P.J., Anderson, A.P., Kopalle, H.M., Banham, A.H., and Partch, C.L. (2015). Cancer/testis antigen PASD1 silences the circadian clock. Mol. Cell *58*, 743–754.

Moglich, A., Ayers, R.A., and Moffat, K. (2009). Structure and signaling mechanism of Per-ARNT-Sim domains. Structure *17*, 1282–1294.

Murshudov, G.N., Vagin, A.A., and Dodson, E.J. (1997). Refinement of macromolecular structures by the maximum-likelihood method. Acta Crystallogr. D Biol. Crystallogr. *53* (pt3), 240–255.

Nagoshi, E., Sugino, K., Kula, E., Okazaki, E., Tachibana, T., Nelson, S., and Rosbash, M. (2010). Dissecting differential gene expression within the circadian neuronal circuit of *Drosophila*. Nat. Neurosci. *13*, 60–68.

Nangle, S.N., Rosensweig, C., Koike, N., Tei, H., Takahashi, J.S., Green, C.B., and Zheng, N. (2014). Molecular assembly of the period-cryptochrome circadian transcriptional repressor complex. Elife *3*, e03674.

Otwinowski, Z., and Minor, W. (1997). Processing of X-ray diffraction data collected in oscillation mode. Methods Enzymol. *276*, 307–326.

Radhakrishnan, I., Perez-Alvarado, G.C., Parker, D., Dyson, H.J., Montminy, M.R., and Wright, P.E. (1997). Solution structure of the KIX domain of CBP bound to the transactivation domain of CREB: a model for activator:coactivator interactions. Cell *91*, 741–752.

Rey, G., Cesbron, F., Rougemont, J., Reinke, H., Brunner, M., and Naef, F. (2011). Genome-wide and phase-specific DNA-binding rhythms of BMAL1 control circadian output functions in mouse liver. PLoS Biol. *9*, e1000595.

Schmalen, I., Reischl, S., Wallach, T., Klemz, R., Grudziecki, A., Prabu, J.R., Benda, C., Kramer, A., and Wolf, E. (2014). Interaction of circadian clock proteins CRY1 and PER2 is modulated by zinc binding and disulfide bond formation. Cell *157*, 1203–1215.

Schuck, P. (2000). Size-distribution analysis of macromolecules by sedimentation velocity ultracentrifugation and lamm equation modeling. Biophys. J. *78*, 1606–1619.

Sheffield, P., Garrard, S., and Derewenda, Z. (1999). Overcoming expression and purification problems of RhoGDI using a family of "parallel" expression vectors. Protein Expr. Purif. *15*, 34–39.

Takahata, S., Ozaki, T., Mimura, J., Kikuchi, Y., Sogawa, K., and Fujii-Kuriyama, Y. (2000). Transactivation mechanisms of mouse clock transcription factors, mClock and mArnt3. Genes Cells *5*, 739–747.

Wang, F., Marshall, C.B., Yamamoto, K., Li, G.Y., Gasmi-Seabrook, G.M., Okada, H., Mak, T.W., and Ikura, M. (2012). Structures of KIX domain of CBP in complex with two FOXO3a transactivation domains reveal promiscuity and plasticity in coactivator recruitment. Proc. Natl. Acad. Sci. USA *109*, 6078–6083.

Wojciak, J.M., Martinez-Yamout, M.A., Dyson, H.J., and Wright, P.E. (2009). Structural basis for recruitment of CBP/p300 coactivators by STAT1 and STAT2 transactivation domains. EMBO J. *28*, 948–958.

Ye, R., Selby, C.P., Ozturk, N., Annayev, Y., and Sancar, A. (2011). Biochemical analysis of the canonical model for the mammalian circadian clock. J. Biol. Chem. *286*, 25891–25902.

Zhao, W.N., Malinin, N., Yang, F.C., Staknis, D., Gekakis, N., Maier, B., Reischl, S., Kramer, A., and Weitz, C.J. (2007). CIPC is a mammalian circadian clock protein without invertebrate homologues. Nat. Cell Biol. *9*, 268–275.

STAR★METHODS

KEY RESOURCES TABLE

REAGENT OR RESOURCE	SOURCE	IDENTIFIER
Bacterial and Virus Strains		
BL21(DE3)	MilliporeSigma (Novagen)	69,450
BL834(DE3)	MilliporeSigma (Novagen)	69,041
Chemicals, Peptides, and Recombinant Proteins		
SelenoMethionine medium	Molecular Dimensions	Cat# MD12-500
In-fusion HD cloning kit	Takara (Clontech)	Cat# 638910
Critical Commercial assays		
Dual-Luciferase® reporter assay system	Promega	Cat# E1910
Deposited Data		
Crystal structure, mCLOCK Exon19:CIPC $P2_12_12_1$ form	This paper	PDB 5VJI
Crystal structure: mCLOCK Exon19:CIPC C2 form	This paper	PDB:5VJX
Experimental Models: Cell Lines		
Schneider 2 (S2)	Thermo Fisher Scientific	Cat# R69007
Recombinant DNA		
Plasmid: pMBP-Parallel1	(Sheffield et al., 1999)	NA
Plasmid: pcDNA3.1 vector	Thermo Fisher Scientific	V79020
Plasmid: pAC5.1	Thermo Fisher Scientific	V411020
Plasmid: pCMV10/HA-mBMAL1	(Huang et al., 2012)	NA
Plasmid: pCMV10/3xflag-mClock	(Huang et al., 2012)	NA
Plasmid: pGL3-basic	Promega	Cat# E1751
Plasmid: pGL3 Pro E2	Addgene	Plasmid#48749
Plasmid: pAC-dCLK	Addgene	Plasmid#33153
Plasmid: pAC-Cyc	Addgene	Plasmid#33156
Plasmid: pAC-per	Addgene	Plasmid#33157
Software and Algorithms		
HKL3000	(Otwinowski and Minor, 1997)	http://www.hkl-xray.com/hkl-3000
PHENIX	(Adams et al., 2010)	http://www.phenix-online.org/
REFMAC	(Murshudov et al., 1997)	http://www.ccp4.ac.uk/
CCP4	(Collaborative Computational Project, Number 4, 1994)	http://www.ccp4.ac.uk/
PyMOL	Schrödinger, LLC	https://www.pymol.org/
SEDFIT	(Schuck, 2000)	http://www.analyticalultracentrifugation.com/default.htm
GUSSI	UTSW Macromolecular Biophysics Resource	http://biophysics.swmed.edu/MBR/software.html
NMRPipe	(Delaglio et al., 1995)	https://spin.niddk.nih.gov/bax/software/NMRPipe/
NMR View	(Johnson and Blevins, 1994)	http://www.onemoonscientific.com/nmrviewj
Molprobity	(Davis et al., 2004)	http://molprobity.biochem.duke.edu/

CONTACT FOR REAGENT AND RESOURCE SHARING

Further information and requests for resources and reagents should be directed to and will be fulfilled by the Lead Contact, Hong Zhang (zhang@chop.swmed.edu).

EXPERIMENTAL MODEL AND SUBJECT DETAILS

HEK293T Cell Culture

HEK293T cells were grown in DMEM medium with 10% FBS and 1% Penicillin-Streptomycin at 37°C.

Schneider 2 (S2) Cell Culture

S2 cells were grown in Schneider's *Drosophila* medium (Invitrogen) 10% FBS and 1% Penicillin-Streptomycin at 28°C.

METHOD DETAILS

Protein Expression, Purification, and Crystallization

The Exon19 domain (517–560) of mouse CLOCK and 6xHis tagged mouse CIPC CLOCK-binding domain (317–379) with upstream T7 *lac* DNA sequence were cloned into pMBP-Parallel1 plasmid (Sheffield et al., 1999), and coexpressed in BL21 (DE3) *E. coli* cells. Harvested cells were lysed by a pressure homogenizer in a buffer containing 50 mM NaH_2PO_4, pH8.0, 300 mM NaCl, 20 mM imidazole, 5 mM β-mercaptoethanol, 1 mM PMSF, and 0.03% (v/v) Brij-35. The clarified cell lysate was incubated with His60 Ni beads (Clontech) at 4°C for one hour, and the bound protein was eluted with liner gradient of 20-500mM imidazole. The pooled fractions were buffer exchanged into 50 mM MES, pH5.5, 50 mM NaCl, 2mM DTT. The MBP and 6xHis tags were removed by TEV protease overnight at room temperature. The CLOCK Exon19:CIPC complex was further purified using a HiTrap SP column (GE Healthcare Life Sciences) followed by Superdex75 gel filtration chromatography (GE Healthcare Life Sciences) and eluted in 50 mM MES pH5.5, 100 mM NaCl, and 2 mM DTT. The protein was then concentrated to 25mg/ml, aliquoted, and flash frozen in liquid nitrogen and stored in −80°C. The Exon19 domain of *Drosophila melanogaster* CLOCK (AAS65057.2, residues 526–570) and CIPC homolog (AAF56571.2, residues 190–264) were coexpressed and purified using a similar procedure.

N^{15} labeled mouse Exon19:CIPC was expressed in BL21 (DE3) *E. coli* cells in M9 medium supplemented with 2mM $MgSO_4$, 0.1mM $CaCl_2$, 0.4% (w/v) D-glucose, 0.0005% (w/v) Thiamine and trace element. Selenomethionine (SeMet) labeled CLOCK Exon19:CIPC was expressed in B834 (DE3) cells in the Selenomethionine medium from Molecular Dimensions (catalog number MD12-500). Both labeled proteins were purified with the same procedure as the native protein.

SeMet labeled Exon19:CIPC complex crystals were grown at 20°C using the hanging drop vapor diffusion method. The reservoir solution for Crystal I (spacegroup $P2_12_12_1$) consisted of 100 mM Bis-Tris, pH7.3, 27% PEG2000MME and was mixed with protein in a 1:1 ratio plus a final 0.5% β-Dodecyl Maltoside as additive. For Crystal II (spacegroup C2), the reservoir solution consisted of 100 mM HEPES, pH8.0, 200 mM Proline, 16% PEG3350 and was mixed with protein in a 1:1 ratio. Crystal I was transferred to a cryoprotectant solution of 100 mM HEPES pH7.5, 24% PEG2KMME, and 20% PEG400, and flash frozen in liquid nitrogen. Crystal II was transferred into 100 mM HEPES pH8.0, 200 mM Proline, 15% PEG3350, and 3% myo-Inositol (w/v) before flash frozen in liquid nitrogen.

X-Ray Data Collection, Structure Determination and Analysis

Single wavelength anomalous dispersion (SAD) data from selenomethionine labeled CLOCK Exon19:CIPC were collected to a resolution of 1.86Å (Crystal I) and 2.70Å (Crystal II), respectively, at Beamline 19-ID of Advanced Photon Source (APS), Argonne National Laboratory, Lemont, IL. The diffraction images were integrated, merged and scaled using HKL3000 software package (Otwinowski and Minor, 1997). Selenium heavy atom sites determination, *ab initio* phase determination, density modification, initial model building were performed using PHENIX Suite (Adams et al., 2010). Manual model building was performed using Coot (Emsley et al., 2010). Further structure refinement was performed using REFMAC5 (Collaborative Computational Project, Number 4, 1994) and phenix.refine (Adams et al., 2010). The crystal data and final refinement statistics were summarized in Table 1. All figures were drawn using the program PyMOL (The PyMOL Molecular Graphics System, Version 1.7.4 Schrödinger, LLC)

Analytical Ultracentrifuge

Sedimentation velocity (SV) ultracentrifugation experiments were performed at 20°C in a Beckman ProteomeLab XL-1ultracentrifuge using an An50Ti rotor (Beckman Coulter). 400μl mouse MBP-Exon19:6xHis-CIPC complex in 50 mM NaH_2PO_4,pH 8.0, 100 mM NaCl, and 400μl untagged mouse CLOCK Exon19:CIPC in 50 mM MES pH 5.5, 100 mM NaCl were loaded along with the corresponding reference buffers into the same centerpieces. The rotor was evenly accelerated to 50,000 rpm and both UV absorbance and Rayleigh interference data were collected overnight. The sedimentation coefficient distribution was analyzed by the program SEDFIT (Schuck, 2000) and the graphs were drawn using GUSSI (biophysics.swmed.edu/MBR/software.html).

^{15}N-^{1}H TROSY-HSQC

Two-dimensional ^{15}N-^{1}H TROSY-HSQC spectra were recorded on INOVA600 spectrometers at 33°C using 1 mM sample of ^{15}N-labeled CLOCK Exon19:CIPC complex in a buffer containing 50 mM MES pH5.5, 100 mM NaCl, with 8% D2O. Data was processed using the NMRPipe program (Delaglio et al., 1995) and analyzed with NMRView (Johnson and Blevins, 1994).

Mutagenesis

Point mutations of full-length mouse CIPC, mouse CLOCK, drosophila CIPC, and drosophila CLK were introduced by standard site-directed mutagenesis using the QuickChange II Site-Directed Mutagenesis Kit (Agilent Technologies). Briefly, mixtures of mutagenic

primers, the corresponding plasmids encoding wt CIPC or CLOCKs, 10X reaction buffer, dNTP mix, and *Pfu Ultra* HF DNA polymerase, were prepared and subjected to thermal cycling for 18 cycles. *Dpn* I restriction enzyme was added directly to each amplification reaction and each reaction was incubated at 37°C for 1 hr. The mutated coding DNAs were transformed into competent cells for nick repair. DNA sequencing was performed to select the correct point mutations.

Transactivation Assays

cDNAs encoding full-length mouse CIPC and drosophila CIPC were amplified using standard PCR technique. Full-length mouse CIPC cDNA was subsequently inserted into pcDNA3.1 (+) vector between Hind III restriction site using the In-fusion HD cloning kit (Clontech). Full-length drosophila CIPC cDNA was inserted into pAc5.1 vector between KpnI and XhoI restriction sites with T4 DNA ligase (NEB).

HEK293T cells were grown in DMEM medium with 10% FBS and 1% Penicillin-Streptomycin. Cells were plated in 96-well plates the day before transfection at 4 X 10^4 cells per well. Cells were transfected with 10 ng mouse *Per2*-promoter driven luciferase reporter plasmid (Addgene #48749), 2 ng SV40-Renilla plasmid (Promega) for normalization, and 63 ng plasmid each for CLOCK (Huang et al., 2012) (or CLOCK mutant), BMAL1 (Huang et al., 2012), CIPC (or CIPC mutant), or CRY1 (Huang et al., 2012). The transfection was performed using lipofectamine 2000 (Invitrogen) according to the manufacturer's protocol. The total amount of DNA transfected was held at about 200 ng in each transfection reaction. 48 hours after transfection, cells were lysed and the luciferase activity was measured from 20 μL of lysate using the Dual-Luciferase Reporter Assay System (Promega).

Drosophila Per-promoter driven firefly luciferase reporter vector was constructed by cloning the 69-bp DNA fragment upstream of the *Per* gene (Hao et al., 1997) into pGL3-basic vector (Promega) between XhoI and HindIII restriction sites. Schneider 2 cells were grown in Schneider's *Drosophila* medium (Invitrogen) with 10% FBS and 1% Penicillin-Streptomycin. Cells were plated in 12-well plates the day before transfection at 1 X 10^6 per well. Cells were transfected with 1 μg *Drosophila Per*-promoter driven luciferase reporter plasmid, 50 ng PolIII-renilla plasmid, 1 μg plasmid each for *Drosophila* CLOCK (Addgene #33153), CYC (BMAL1 ortholog, Addgene #33156), CIPC or PER (Addgene #33157). The transfection was performed using the Calcium Phosphate Transfection Kit (Invitrogen) according to the manufacturer's protocol. The total amount of DNA transfected in each reaction was held at about 4 μg. 48 hours after transfection, cells were spun down and lysed. The luciferase activity was measure from 50 μL of lysate using the Dual-Luciferase Reporter Assay System (Promega).

DATA AND SOFTWARE AVAILABILITY

Atomic coordinates and structure factors for the reported crystal structures have been deposited in the PDB under ID codes 5VJI ($P2_12_12_1$ space group) and 5VJX (C2 space group).